

N86-32370

74

## SIMULATION OF COSMIC IRRADIATION CONDITIONS IN THICK TARGET ARRANGEMENTS

S.Theis, P.Englert, Institut für Kernchemie der Universität zu Köln, Zülpicher Str. 47, D-5000 Köln-1, W.-Germany; R.C.Reedy, INC-11, Los Alamos, National Laboratory, Los Alamos, NM 87545, USA; J.R.Arnold, University of California, San Diego, Department of Chemistry, La Jolla, Ca 92093, USA.

Interpreting abundances of cosmogenic nuclides in meteorites, planetary atmospheres and surfaces in terms of exposure history, shielding parameters and cosmic ray flux requires knowledge of the nuclear reactions that produce them in the object or environment considered.

Bombardment experiments with thin and thick targets with energetic charged particles or particle fields have been performed in order to gain a pool of production data (production rates, ratios, cross sections) for cosmogenic nuclides [1,2,3], of which the stable and the long-lived radioactive species are of special interest as they have been measured in many extraterrestrial samples and are used in evaluating the exposure ages and histories of these bodies [4,5]. In order to correlate the simulation experiments with the systematics of spallogenic nuclide production during exposure to the galactic cosmic radiation, it is necessary to determine long-lived radionuclides as well as stable isotopes in targets from such experiments.

An important point in thick target experiments is to transform the available beam geometry to the isotropic irradiation conditions in space. This can be done by mathematical transformations of the data obtained from static thick targets exposed to focussed monoenergetic beams [6], by defocussing the beam and moving the target in the beam line during the irradiation [7] or by using secondary particle fields for the irradiation as they occur in the interior of extraterrestrial objects [8].

nuclide	$T_{1/2}$	decay mode	carrier amount[mg]	chemical yield[%]	detection method
Be-7	53.29 d	$\epsilon$	1-2	80-90	G, $E_{\gamma} = 478$ keV
Be-10	$1.6 \times 10^6$ a	$\beta^{-}$	1-2	80-90	AMS
Na-22	2.607 a	$\beta^{+}$	0.05-0.1	99.99	G, $E_{\gamma} = 1275$ keV
Al-26	$7.16 \times 10^6$ a	$\beta^{+}$	$\sim 2$	60-95	GGC, AMS
Ti-44	47.3 a	$\epsilon$	$\sim 4$	90-95	G, GGC (via Sc-44)
Mn-54	312.2 d	$\epsilon$	$\sim 3$	80-85	G, $E_{\gamma} = 835$ keV
Co-56	78.76 d	$\epsilon, \beta^{+}$	instrumental		G, $E_{\gamma} = 847, 1238$ KeV
Co-57	271.3 d	$\epsilon$	instrumental		G, $E_{\gamma} = 122, 136$ keV
Co-58	70,78 d	$\epsilon$	instrumental		G, $E_{\gamma} = 811$ keV
Co-60	5.272 a	$\beta^{-}$	instrumental		G, $E_{\gamma} = 1173, 1332$ keV

Table 1: Nuclear properties of radionuclides determined in this study. In columns 4 and 5 carrier amounts and chemical yields of the applied separation procedures are listed. The determination methods in column 6 are: G: high resolution (low-level)  $\gamma$ -spectroscopy, GGC:  $\gamma$ - $\gamma$ -coincidence spectroscopy, AMS: accelerator mass spectroscopy.

\*

C-2

## SIMULATION OF COSMIC IRRADIATION

Theis, S. et al.

This study is dedicated to the analysis of long-lived cosmogenic radionuclides produced in pure elemental targets during various simulation experiments by using pure instrumental as well as radiochemical methods (see table 1). The nature of the chemical purification procedures depend on the isotope to be separated, the target material, the interfering isotopes present, and the detection method. Some examples of the applied separation schemes have been published previously [8,9]. In all experiments short-lived isotopes were determined prior to chemistry in most of the target elements by high resolution  $\gamma$ -spectroscopy.

A first set of production data was obtained from a high energy neutron ( $E_n \leq 800$  MeV) irradiation at several positions under the LAMPF beam stop (Los Alamos Meson Physics Facility) and is given in table 2. The beam stop environment produces secondary particle and especially neutron fields, which resemble those in planetary surfaces (depth  $>180$  g/cm<sup>2</sup>) exposed to the GCA [8]. The samples were exposed in three positions with different absolute neutron fluxes and spectral hardness [9].

The nuclide Ti-44 ( $T_{1/2} = 47,3$  a) was measured in Ti-targets where it is produced via (n,xn) reactions from all stable Ti isotopes (Ti-46,47,48,49,50). The main target isotope, however, is Ti-48 (73.8 %), which contributes via a (n,5n) reaction to the Ti-44 activity. Compared to the (n,4n) product Co-56 from the monoisotopic Co-59 the Ti-44 production rates are one order of magnitude lower for the respective irradiation positions.

Ti-44 could be of special interest in lunar surface samples. It is produced by SCR reactions in the upper layers and - because of its half-life - able to monitor the mean solar activity for at least 4-5 eleven-year solar

product	sample location			ref.
	2001	2005	2006	
	[accum. atoms g <sup>-1</sup> ]			
Al-26(Al)	1.3x10 <sup>14</sup>	6.4x10 <sup>13</sup>	4.1x10 <sup>13</sup>	[9]
Na-22(Al)	3.2x10 <sup>13</sup>	1.7x10 <sup>13</sup>	8.8x10 <sup>12</sup>	[9]
Be- 7(Al)	1.2x10 <sup>12</sup>	6.7x10 <sup>11</sup>	3.8x10 <sup>11</sup>	[9]
Co-60(Co)	4.4x10 <sup>15</sup>	1.7x10 <sup>16</sup>	2.1x10 <sup>16</sup>	
Co-58(Co)	3.0x10 <sup>14</sup>	1.8x10 <sup>14</sup>	1.0x10 <sup>14</sup>	
Co-57(Co)	1.0x10 <sup>14</sup>	5.7x10 <sup>13</sup>	3.9x10 <sup>12</sup>	
Co-56(Co)	1.6x10 <sup>13</sup>	8.3x10 <sup>12</sup>	---	
Ti-44(Ti)	1.6x10 <sup>12</sup>	1.2x10 <sup>12</sup>	5.2x10 <sup>11</sup>	
Na-22(Ti)	---	1.2x10 <sup>11</sup>	4.9x10 <sup>10</sup>	
Be- 7(Ti)	---	1.8x10 <sup>11</sup>	5.5x10 <sup>10</sup>	
Be- 7(Fe)	2.0x10 <sup>11</sup>	1.4x10 <sup>11</sup>	---	[9]
Na-22(Ni)	2.6x10 <sup>10</sup>	1.8x10 <sup>10</sup>	6.5x10 <sup>9</sup>	[9]

**Table 2:** Production of low and high energy products in various targets (target elements in brackets) in different irradiation positions under the LAMPF beam stop. For comparison selected results of instrumentally determined Co-isotopes are given.

cycles. As demonstrated, another very important source of Ti-44 in lunar samples are reactions of high energy secondary neutrons with Ti, which has an abundance of several % in the moon [10]. These reactions can occur in greater depths, where the lunar secondary particle cascade is well developed. Here spallation production in iron is of less significance.

Another approach to simulate 2- $\pi$  irradiation conditions of planetary surfaces which has been widely applied in the past are bombardments of so called thick targets [11]. A very large thick target was exposed recently to

## SIMULATION OF COSMIC IRRADIATION

Theis, S. et al.

2.1 GeV protons at the Bevatron-Bevalac in Berkeley [12]. In a 100x100x180 cm steel surrounded granodiorite target radioactive medium and high energy spallation products of the incident primary and of secondary particles were analyzed along the beam axis down to depths of 140 g/cm<sup>2</sup> in targets such as Cu, Ni, Co, Fe, Ti, Si, SiO<sub>2</sub> and Al. Activities of these nuclides were exclusively determined via instrumental  $\gamma$ -ray spectroscopy. Figure 1 shows relative yields of neutron capture and spallation products induced in Co and Cu targets during the thick target bombardment as a function of depth. The majority of the medium energy products such as Co-58 from Co targets exhibit a maximum at shallow depths of 40-60 g/cm<sup>2</sup> and then decrease exponentially.

In a comparable 600 MeV proton bombarded thick target such a slight maximum for medium energy products was not observed [13]. Rather, Co-58 activities in Co decreased steadily with the highest activity at the surface.

The activities of the n-capture product Co-60 increase steadily starting at the surface. This indicates the rapidly growing flux of low energy neutrons ( $E_n \leq 1$  keV) within the target. The maximum of the low energy neutron distribution lies between 130 and 170 g/cm<sup>2</sup> [12], which is significantly deeper than in the 600 MeV proton bombarded artificial lunar regolith [3]. Be-7 activities representing high energy spallation in Co decrease, as expected, exponentially with depth.

The comparison of the two experiments shows that both, experimental arrangement and incident particle energy have a significant influence of the results obtained. To gain more insight in the development of secondary particle fluxes within planetary surfaces which are exposed to an energetically diverse particle field, results of both simulation experiments will be discussed in detail.

References: [1] e.g. R.Michel et al., 1978, *J.Inorg.Nucl.Chem.* **40**, 1845; [2] R.C.Reedy et al., 1979, *Earth Planet. Sci.Lett.* **44**, 341; [3] R.Michel et al., 1974, *Radiochim.Acta* **21**, 169; [4] P.Englert et al., 1978, *Geochim.Cosmochim.Acta* **42**, 1635; [5] S.Regnier et al., 1983, *Meteoritics* **18**, 384; [6] M.Honda, 1962, *J.Geophys.Res.* **67**, 4847; [7] R.Michel et al., 1984, *Lun.Planet.Sci. Conf. XV*, 542; [8] P.Englert et al., 1983, *Lun.Planet.Sci. Conf. XIV*, 175; [9] S.Theis et al., 1984, *Lun.Planet. Sci.Conf. XV*, 855; [10] R.W.Perkins et al., 1970, *Proc.Apollo 11 Lun.Sci.Conf.*, 1455; [11] T.B.Kohmann et al., 1967, In: *High Energy Nuclear Reactions in Astrophysics*, Benjamin, New York, 169; [12] P.Englert et al., 1983, *Meteoritics* **18**, 294; [13] H.Weigel et al., 1974, *Radiochim.Acta* **21**, 179.

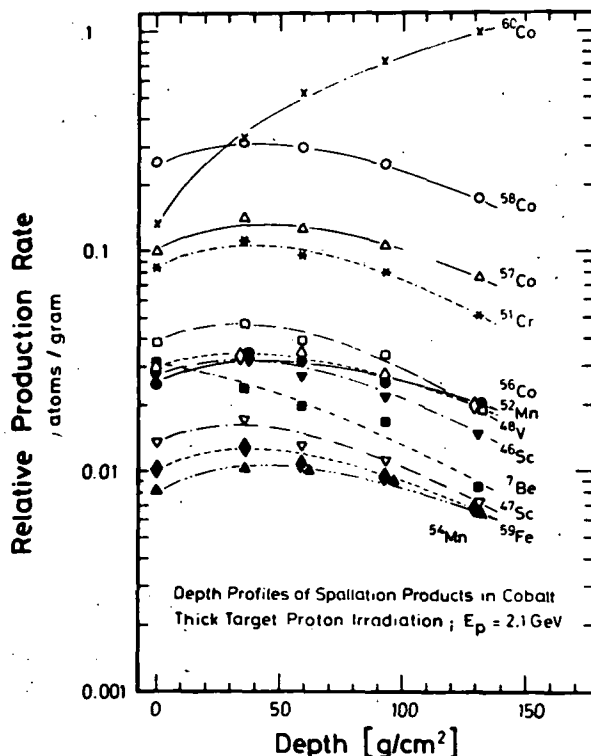


Figure 1